

## Original Research

# Effects of *Corynebacterium bovis* on Engraftment of Patient-derived Chronic Myelomonocytic Leukemia Cells in NSGS Mice

Alexis R Vedder,<sup>1\*</sup> Emily L Miedel,<sup>2</sup> Natalie H Ragland,<sup>2</sup> Maria E Balasis,<sup>1</sup> Christopher T Letson,<sup>1</sup> Robert W Engelman,<sup>2</sup> and Eric Padron<sup>1</sup>

Modeling chronic myelomonocytic leukemia (CMML) in immunodeficient NSGS mice relies on unique human CMML specimens and consistent murine engraftment. Only anecdotal comments have thus far supported the notion that research data may be altered by *Corynebacterium bovis*, an opportunistic cutaneous pathogen of immunodeficient mice. *C. bovis* disseminated by asymptomatic and clinically affected mice with hyperkeratotic dermatitis, resulting in resilient facility contamination and infectious recurrence. Herein we report that, compared with *C. bovis* PCR-negative counterparts, *C. bovis* PCR-positive NSGS mice developed periocular and facial hyperkeratosis and alopecia and had reduced metrics indicative of ineffective human CMML engraftment, including less thrombocytopenia, less splenomegaly, fewer CMML infiltrates in histopathologic sections of murine organs, and fewer human CD45<sup>+</sup> cells in samples from murine spleen, bone marrow, and peripheral blood that were analyzed by flow cytometry. All CMML model metrics of engraftment were significantly reduced in the *C. bovis* PCR-positive cohort compared with the -negative cohort. In addition, a survey of comprehensive cancer center practices revealed that most murine facilities do not routinely test for *C. bovis* or broadly decontaminate the facility or its equipment after a *C. bovis* outbreak, thus increasing the likelihood of recurrence of invalidated studies. Our findings document that CMML engraftment of NSGS mice is diminished—and the integrity of murine research data jeopardized—by *C. bovis* infection of immunodeficient mice. In addition, our results indicate that *C. bovis* should be excluded from and not tolerated in murine facilities housing immunodeficient strains.

**Abbreviations:** CMML, chronic myelomonocytic leukemia; NCI, National Cancer Institute; PDX, patient-derived xenograft; VHP, vaporized hydrogen peroxide

DOI: 10.30802/AALAS-CM-18-000138

Chronic myelomonocytic leukemia (CMML) is an aggressive myeloid malignancy of older adults that is associated with a median survival of 34 mo and features of myeloproliferative neoplasm and myelodysplastic syndrome.<sup>2,21</sup> As such, patients with CMML present with significant clinical heterogeneity, including cytopenia, leukocytosis, splenomegaly, peripheral monocytosis, and bone marrow dysplasia.<sup>1,3</sup> Somatic mutations are identified in more than 90% of patients with CMML, predominantly altering epigenetic, splicing, and cytokine signaling pathways.<sup>10,22</sup> Allogeneic stem cell transplantation is the only potentially curative therapy, although many patients are often ineligible due to age or comorbidities.<sup>2,9,21</sup> Efforts to model CMML by creating genetically engineered mouse models that carry the highly recurrent mutations found in human CMML, either alone or in combination, have not recapitulated the unique clinical heterogeneity or clonal genetic composition of the disease.<sup>1,12,13,19,23</sup> In light of the mutational and clinical variability of patients with CMML, we recently evaluated CMML primary bone marrow samples in vitro and observed that GM-CSF hypersensitivity

was a convergent molecular phenotype of this disease.<sup>20</sup> These findings, and the absence of established CMML cell lines or murine models, led us to develop a CMML patient-derived xenograft (PDX) model using the triple transgenic NOD.Cg-Prkdcscid Il2rgtm1Wjl Tg(CMV-IL3,CSF2,KITLG)1Eav/MloySzJ (NSG-SGM3, NSGS) mice, which express human IL3, GM-CSF, and stem cell factor.<sup>30</sup>

In our prior report of this CMML mouse model, we demonstrated that sublethally irradiated NSGS mice are engrafted by CMML primary PDX as purified CD34<sup>+</sup> cells, unfractionated bone marrow, or PBMC, resulting in splenomegaly, thrombocytopenia, and immunohistochemically localizable CMML infiltrates in the bone marrow, spleen, liver, and lung of engrafted NSGS mice and thus recapitulating the human condition.<sup>31</sup> This CMML PDX mouse model was found to be genetically and phenotypically accurate, with serially transplanted PDX cells in NSGS mice remaining similar to the original immunophenotype, morphology, and genetic mutations of the CMML patient.<sup>31</sup> This new mouse model permits the characterization of CMML disease pathogenesis and the testing of novel CMML therapeutics but is limited by the rarity of CMML patient specimens for NSGS mouse engraftment. As a consequence, there is no room for error or tolerance for study invalidation

Received: 26 Nov 2018. Revision requested: 23 Jan 2019. Accepted: 08 Feb 2019.  
Departments of <sup>1</sup>Malignant Hematology and <sup>2</sup>Comparative Medicine, H Lee Moffitt  
Cancer Center & Research Institute, University of South Florida, Tampa, Florida  
<sup>\*</sup>Corresponding author. Email: alexis.vedder@moffitt.org

by opportunistic microbes when working with unique human CMML patient PDX NSGS mouse models.

We have also recently reported that the integrity of data derived from immunodeficient mice acquired in a topographically complex research setting relies on enhanced biosecurity measures, including monitoring for opportunistic microbes and the regular implementation of a validated room and equipment sterilization method.<sup>18,24,25</sup> To this end, we developed procedures for sterilizing murine IVC racks and air-handling units by using vaporized hydrogen peroxide (VHP) and PCR monitoring.<sup>24</sup> We then applied this method of PCR environmental and murine monitoring and VHP equipment and room sterilization to the first documented facility-wide eradication of *Corynebacterium bovis*.<sup>18</sup> In addition, we documented the PCR prevalence and VHP mitigation of a broad spectrum of murine opportunistic microbes, including *Staphylococcus xylosum*, *Proteus mirabilis*, and *Pasteurella pneumotropica biotype Heyl*.<sup>25</sup> During the development of these PCR testing and *C. bovis* eradication methods, we surveyed the attending veterinarians of other SPF and viral antibody-free murine facilities based at National Cancer Institute (NCI)-designated Comprehensive Cancer Centers and herein report the *C. bovis* monitoring and mitigation practices at these institutions.

Furthermore, although *C. bovis* is known to cause hyperkeratotic acanthotic dermatitis in nude mice and skin disease in haired *Pkrdc<sup>scid</sup>* mice and hairless immunocompetent SKH1-Hrhr mice, can be transmitted in resected PDX or allograft tumors, results in broad facility contamination, and can be eradicated by PCR testing and VHP sterilization,<sup>3-5,16-18,27</sup> only anecdotal comments have thus far supported the notion that research data may be altered due to *C. bovis* infection of immunodeficient mice.<sup>6,15,27</sup> Consequently, during the development of methods resulting in the first facility-wide eradication of *C. bovis*,<sup>18</sup> we also monitored cohorts of CMML PDX-recipient NSGS mice, some of which exhibited periocular alopecia, for evidence of CMML engraftment and for *C. bovis* status. Murine and environmental specimens representative of these CMML PDX recipients were PCR-evaluated for *C. bovis*, and mice were monitored to IACUC-approved clinical endpoints for CMML PDX engraftment. Herein, we describe the first documentation of the influence of *C. bovis* infection of immunodeficient mice on research data obtained from those animals.

## Materials and Methods

**Murine facility.** The H Lee Moffitt Cancer Center and Research Institute is Florida's only NCI-designated Comprehensive Cancer Center. Its 350,000 nominal ft<sup>2</sup> Stabile Research Building houses a 29,931 ft<sup>2</sup> vivarium comprising 7117 ft<sup>2</sup> of murine housing space outside of quarantine and 4510 ft<sup>2</sup> of procedural, surgical, imaging, irradiation, and murine genetic engineering space. The program and facilities for animal care and use are fully AAALAC-accredited, and all animals were housed and used in accordance with IACUC-approved protocols.

The Stabile Research Building is an SPF, viral antibody-free murine facility with a separate quarantine that is located outside of the murine facility proper. Quarantine and sentinel testing standard procedures exclude murine norovirus, *Helicobacter spp.*, *Syphacia spp.*, *Aspicularis tetraptera*, *Parainfluenza virus type 1* (Sendai), coronavirus (mouse hepatitis virus), *Mycoplasma pulmonis*, paramyxovirus (pneumonia virus of mice), parvovirus (minute virus of mice and mouse parvovirus), poliovirus (Theiler murine encephalomyelitis virus, GDVII strain), reovirus type 3, lymphocytic choriomeningitis virus, *Mouse adenovirus types 1 and 2*, poxvirus (ectromelia virus), rotavirus (epizootic diarrhea

of infant mice virus), papovavirus (polyoma virus), Hantaan virus, cilia-associated respiratory bacillus, *Clostridium piliforme* (Tyzzer disease), and *Encephalitozoon cuniculi*. At the time of the present report, no standard procedures to exclude or to monitor and not tolerate *C. bovis* were in place.<sup>18</sup>

**Mice.** NSGS mice (stock no. 013062, The Jackson Laboratory, Bar Harbor, ME) were purchased and used to establish an intramural colony. Individual mice from this intramural NSGS colony were reassigned to an IACUC-approved research protocol to serve as recipients for CMML PDX engraftment. An outbreak of *C. bovis* in the Stabile Research Building was first recognized in October 2016. Prior to the depopulation of all *C. bovis* PCR-positive immunodeficient mice, and the VHP decontamination of all facility rooms and equipment,<sup>18</sup> we assessed murine recipients of CMML PDX for CMML engraftment and PCR-monitored these mice, IVC rack exhaust plenums, and IVC primary enclosures used to house these mice for *C. bovis* until the completion of study at clinical endpoints. Mice were housed in IVC microisolation caging (Blueline, Tecniplast, Buguggiate, Italy) in a doubled-sided IVC rack configuration, with HEPA-filtered air supplied and exhausted by separate, mobile air-handling units (SmartFlow, Tecniplast).

**PCR surveillance for *C. bovis*.** Sterile FLOQ swabs (Copan Flock Technologies, Brescia, Italy) were used to collect environmental specimens from equipment surfaces by tracing a circular pattern for 3 circumferences as the tip was rolled. Swabs of IVC rack exhaust plenums or IVC primary enclosures or fecal pellets of mice were submitted to an outside laboratory (IDEXX BioResearch, Columbia, MO) for *C. bovis* real-time PCR testing;<sup>18</sup> this assay targets a region of the 16S rRNA gene that is conserved among all *C. bovis* genomic sequences deposited in GenBank and uses a FAM/TAMRA-labeled hydrolysis probe. Hydrolysis probe-based real-time PCR assays targeting the bacterial gene (16S rRNA) were used to ensure DNA recovery and the absence of PCR inhibitors in extracted nucleic acids. Real-time PCR analysis was performed by using standard primer and probe concentrations and a master mix (LC480 ProbesMaster, Roche Applied Science, Indianapolis, IN) on a real-time PCR platform (LightCycler 480, Roche).

Fecal pellets representative of individual CMML PDX-recipient NSGS mice, swabs of each IVC interior, and swabs of each IVC rack exhaust plenum interior were collected and PCR-analyzed, to ensure that *C. bovis*-infected mice and cages were grouped together and were separate from *C. bovis*-unaffected IVC cages and mice. Mice were housed in the same housing room for the duration of study, but IVC were opened only inside a class II A2 biosafety cabinet after surface decontamination with chlorine dioxide spray (Clidox, Pharmacal, Naugatuck, CT) followed by a 70% ethanol rinse. Serial *C. bovis* PCR monitoring of 153 specimens from the 60 mice, the 13 IVC interiors in which mice were housed on 2 IVC racks, and the 2 IVC exhaust plenums continued through the CMML PDX study until clinical endpoints were reached and the CMML PDX-recipient NSGS mice were euthanized. The *C. bovis* status of each cohort did not change during the study. Mice that lost more than 20% of their original body weight (measured twice weekly) or that presented with reduced activity, failure to groom, isolation from cagemates, lack of inquisitiveness, or a hunched posture were euthanized. Mice that presented with these IACUC-approved preterminal clinical endpoints were euthanized by carbon dioxide inhalation followed by a secondary physical method of euthanasia, in accordance with the IACUC-approved protocol.

**PDX.** Human diagnostic bone marrow or peripheral blood specimens were obtained from CMML patients after written

informed consent was obtained in accordance with an Institutional Review Board–approved protocol. Unfractionated bone marrow or peripheral blood mononuclear cells of human patients with CMML were used as PDX and administered to irradiated NSGS mice. For xenotransplantation, NSGS mice ( $n = 60$ ; age, 6 to 10 wk) were sublethally irradiated with 250 cGy by using a Cs<sup>137</sup> source (Mark I Gamma Irradiator, JL Shephard, San Fernando, CA) on the day before PDX transplantation. The following morning, each of the NSGS mice received 1 to 4 × 10<sup>6</sup> human CMML mononuclear cells by tail-vein injection. Mice were monitored twice daily and weighed at least 3 times weekly. Peripheral blood samples collected from recipient NSGS by cardiocentesis at endpoint underwent CBC analysis (IDEXX Veterinary Diagnostics). This method of CMML PDX modeling results in premoribund euthanasia of CMML PDX-recipient NSGS mice at approximately 30 to 120 d after injection and is preceded by thrombocytopenia in engrafted mice.<sup>31</sup>

After euthanasia of CMML PDX-recipient NSGS mice, tissues including blood, spleen, liver, lung, femora, and tibiae were collected for analyses. Spleens were weighed. Mononuclear cells were isolated from peripheral blood, bone marrow, and spleen and analyzed by flow cytometry to determine the degree of human CD45<sup>+</sup> chimerism in each murine tissue. In addition, mononuclear cells isolated from the bone marrow, spleen, and peripheral blood were stained with Zombie Violet (ThermoFisher Scientific, Waltham MA) to confirm cell viability, fixed with 1.6% formaldehyde, and stained with the following antibodies. For MNC specimen surface staining, we used BUV737 mouse antimouse CD45.1 (BD Biosciences, San Jose, CA), a monoclonal antibody that specifically binds to the leukocyte common antigen of mice; BV605 mouse antihuman CD45 (BD Biosciences), a monoclonal antibody that specifically binds to the leukocyte common antigen of humans; and human CD3 APC (BD Biosciences), which binds the  $\epsilon$  chain of the CD3 antigen–T-cell antigen receptor complex of human thymocytes. All samples were evaluated by using flow cytometry (model LSRII, BD Biosciences), and FACS data were analyzed by using FloJo software (version 10, FloJo, Ashland, OR). In addition, lung, spleen, liver, and bone marrow samples were fixed in 10% neutral buffered formalin, dehydrated, embedded in paraffin, sectioned at 4  $\mu$ m, and stained with hematoxylin and eosin for histopathology.

**Statistics.** Unpaired  $t$  tests were performed by using Prism 7 (GraphPad Software, La Jolla, CA) to compare numbers of circulating platelets and neutrophils in CMML PDX-recipient NSGS mice and postmortem spleen weights and percentages of human CD45<sup>+</sup> mononuclear cells in spleen, bone marrow, and peripheral blood. Significance was defined as a  $P$  value of 0.05 or lower.

**Survey of *C. bovis* practices.** Survey questions were developed with the assistance of the Survey Methods Core (H Lee Moffitt Cancer Center). During the first quarter of 2017, surveys were emailed to attending veterinarians overseeing murine colonies at each of 50 NCI-designated Comprehensive Cancer Centers. The survey questionnaire asked: (1) What type of mice (for example, immunocompetent strains, immunodeficient strains, or both) do you have in your vivarium? (2) Has your husbandry or care staff seen any clinical cases of *Corynebacterium bovis* in the last year? If so, what do you do with a positive case (for example, treat, quarantine, or cull affected animals)? (3) Do you decontaminate housing rooms or procedural rooms after a *C. bovis* case? If so, how do you decontaminate? (4) Do you screen biologics for *C. bovis*? (5) Do you include *C. bovis* in your sentinel program? If so, what is your practice?

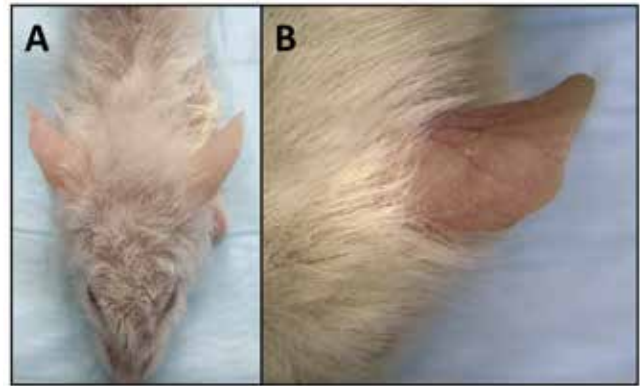


**Figure 1.** (A) Alopecia and scaly skin and (B) an alopecic and scaly ear pinna of a *C. bovis* PCR-positive CMML PDX-recipient NSGS mouse.

## Results

We monitored the *C. bovis* status of 60 CMML PDX-recipient NSGS mice housed in 13 IVC primary enclosures for 87 d by using PCR evaluation of murine fecal pellets and swab specimens collected from each IVC primary enclosure and the exhaust plenum of each IVC rack used to house the mice as separate *C. bovis*-affected or -unaffected cohorts. Most (that is, 39 of 60) of the mice remained asymptomatic and *C. bovis*-PCR negative throughout the 87-d study, whereas the remaining 21 mice developed hyperkeratosis and remained persistently *C. bovis* PCR-positive through study clinical endpoints and euthanasia. Initially, clinically affected mice presented with hyperkeratosis along the face and dorsum, with moderate periocular alopecia. The alopecia of affected mice then spread to the rest of the face, ear pinnae, and dorsum (Figure 1). This presentation of CMML PDX-recipient mice initially appeared clinically similar to cutaneous manifestations of graft-versus-host disease, but mice lacked histopathology of the skin, liver, and small intestine that was consistent with GVHD. Mice were monitored carefully twice daily. Peripheral CBC analysis at endpoint revealed significantly ( $P = 0.0192$ ) greater thrombocytopenia in the *C. bovis* PCR-negative mice compared with the *C. bovis* PCR-positive mice (Figure 2), indicative of greater human CMML PDX engraftment in the *C. bovis*-unaffected cohort. In addition, CBC analysis demonstrated significantly ( $P = 0.0002$ ) more neutrophils in the *C. bovis* PCR-positive mice compared with the *C. bovis* PCR-negative CMML PDX-recipient cohort (Figure 2). All CMML PDX-recipient mice were euthanized at clinical endpoints of study and demonstrated piloerection, hunched posture, reduced activity, and weight loss; tissues were collected for analyses.

After euthanasia, each of the *C. bovis* PCR-positive mice yielded skin specimens that were consistent with the cutaneous pathology of *C. bovis* infection, with each dorsum skin specimen showing an orthokeratotic hyperkeratotic acanthotic dermatitis (Figure 3). *C. bovis*-infected NSGS mice with periocular, facial, and dorsum hyperkeratosis and alopecia did not have noteworthy microscopic abnormalities of the lung, spleen, bone marrow, or liver. Spleen weight was significantly ( $P = 0.0150$ ) greater among the *C. bovis* PCR-negative mice compared with the *C. bovis* PCR-positive mice (Figure 4), consistent with greater human CMML PDX engraftment in the *C. bovis*-unaffected cohort. Even when recipient mice were transplanted with primary samples from the same patient, *C. bovis*-negative mice demonstrated superior engraftment. For example, one mouse that was *C. bovis* PCR-negative was euthanized 34 d after PDX injection and had a spleen weight of 174.3 mg, compared with another mouse

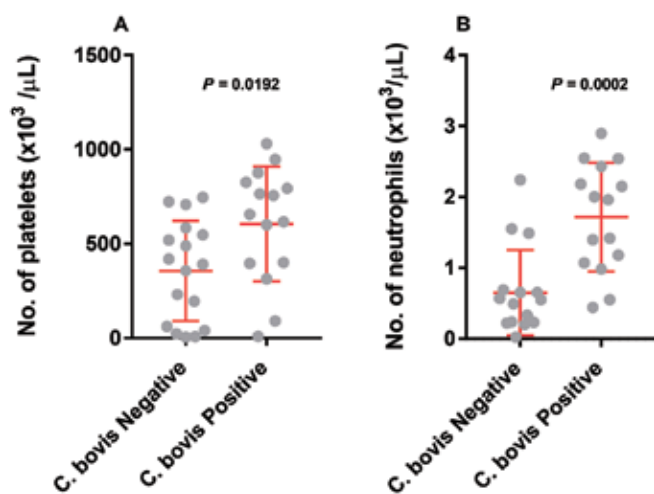


**Figure 2.** Circulating (A) platelet and (B) neutrophil counts of *C. bovis* PCR-negative and -positive CMML PDX-recipient NSGS cohorts.

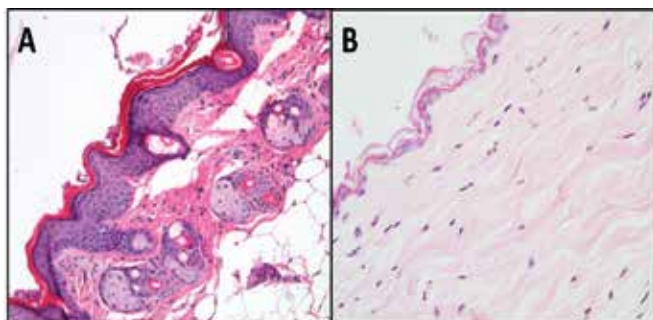


**Figure 3.** Orthokeratotic hyperkeratotic acanthotic dermatitis (A) of a *C. bovis* PCR-positive CMML PDX recipient NSGS mouse compared with (B) the unaffected skin of a *C. bovis* PCR-negative CMML PDX recipient NSGS mouse. Hematoxylin and eosin stain; magnification: 50× (A), 100× (B).

that was *C. bovis* PCR-positive, received the same human PDX isolate, but was euthanized later (at 45 d after PDX injection) and had a substantially lower spleen weight (32.8 mg) at euthanasia (Figure 4 B). This enhanced PDX engraftment of *C. bovis* PCR-negative NSGS mice was supported by the histopathologic evaluation of tissues derived from mice. Human CMML mononuclear cells, including dysplastic cells resembling the human pathologic specimen, were readily noted to have infiltrated the lung, spleen, liver, and bone marrow of *C. bovis* PCR-negative mice but were not present or identified only rarely in *C. bovis* PCR-positive mice (Figure 5). These postmortem impressions were confirmed by the FACS analyses of cells isolated from either the murine spleen, bone marrow, or peripheral blood. Significantly more human CD45<sup>+</sup> cells were present in *C. bovis* PCR-negative murine spleen ( $P = 0.0001$ ), bone marrow ( $P = 0.0034$ ), and peripheral blood ( $P = 0.0440$ ) cell isolates compared with cell specimens isolated from *C. bovis* PCR-positive mice (Figure 6).

Of the 50 questionnaires electronically transmitted to NCI-designated Comprehensive Cancer Centers, 24 (48%) attending veterinarians responded. All cancer center murine facility respondents acknowledged housing both immunocompetent and immunodeficient murine strains, and most respondents (62%) were either unsure (4%) or confirmed having experienced (58%) a clinical case of *C. bovis* hyperkeratotic dermatitis

in immunodeficient mice during the prior year. Most facilities (74%) did not routinely test for *C. bovis* or attempt to exclude the organism from the facility and its murine inventory. During an outbreak, after recognition of a clinical case of *C. bovis* hyperkeratosis, cancer centers relied variously on culling, treating with antibiotics, and quarantining the *C. bovis* clinically affected immunodeficient mice exhibiting hyperkeratosis. Cancer centers equally indicated (25% each) either culling only; culling and treating only; culling and quarantining only; and culling, treating, and quarantining hyperkeratotic immunodeficient mice as practices implemented in response to a *C. bovis* clinical case. Most respondents (52%) were either unsure whether biologics were tested for *C. bovis* in advance of use (9%) or stated that no testing of biologics for *C. bovis* was conducted (43%). A majority of respondents (61%) either were unsure whether any response was implemented (13%), or indicated that no effort was implemented (48%) to decontaminate the *C. bovis*-affected housing or procedural space after an outbreak of *C. bovis*-associated hyperkeratosis. None of the 24 respondents indicated implementing comprehensive environmental and murine surveillance to determine the extent of murine and facility *C. bovis* contamination, followed by the depopulation of all *C. bovis* PCR-positive mice, and the VHP sterilization of all housing and use equipment and facility rooms.

## Discussion

Immunodeficient mice are exquisitely sensitive to opportunistic microbes, including members of the microbiome and emerging pathogens.<sup>7,25,26,29</sup> In addition to the obvious potential for morbidity or mortality, one detrimental drawback of even subclinical infections of immunodeficient mice is the variability induced into research data, normative physiologic responses, and to study metrics, thereby invalidating the findings.<sup>25</sup> When murine studies involve rare, genetically unique human PDX specimens and when experimental therapeutics are available only in limited aliquots, the tolerance for data variability and study invalidation due to opportunistic microbes becomes substantially less. *C. bovis* is a known cause of hyperkeratosis, which manifests clinically in a minority of infected immunodeficient mice, with infection remaining clinically unapparent in many *C. bovis* PCR-positive mice.<sup>3,4,16-18,27</sup> Prior to the present report, merely anecdotal comments supported the notion that *C. bovis* infection alters research data.<sup>6,15,27</sup> Herein, we provide the first documentation of research data being altered by the PCR-confirmed persistence of *C. bovis* infection of immunodeficient mice. This present documentation of altered research study data was conducted during the *C. bovis* outbreak previously described in detail,<sup>18,25</sup> during which *C. bovis* infection of PCR-positive mice was confirmed through both aerobic bacterial culture and microbe identification and by direct visualization of gram-positive rods in histopathologic specimens of skin from immunodeficient mice.

CMML is a lethal hematopoietic malignancy with no available cell lines or methods for culturing primary human cell isolates. Consequently, the CMML PDX mouse model is vital to understanding CMML pathogenesis and to developing improved therapeutic approaches.<sup>31</sup> Metrics indicative of effective human CMML PDX engraftment of NSGS mice include thrombocytopenia, splenomegaly, the presence of CMML infiltrates in histopathologic sections of murine organs, and the presence of CD45<sup>+</sup> cells in FACS-analyzed isolates of murine spleen, bone marrow, and peripheral blood. All of these CMML model metrics were significantly decreased in the *C. bovis* PCR-positive cohort that we describe here. Potentially, increased

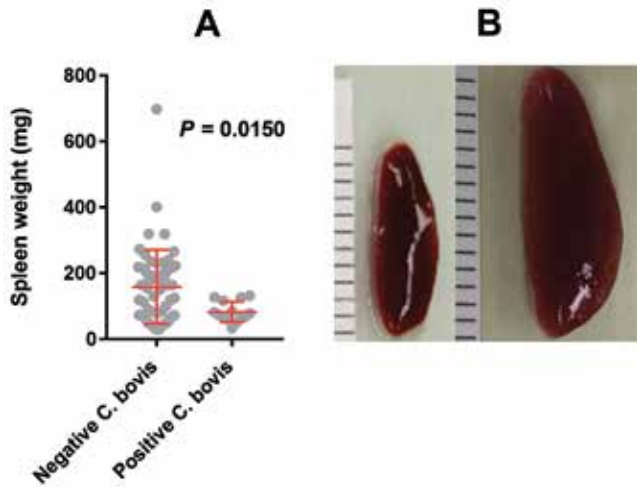


**Figure 4.** (A) Spleen weights of *C. bovis* PCR-negative or -positive CMML PDX-recipient NSGS mice and (B) a representative smaller spleen from a *C. bovis* PCR-positive CMML PDX-recipient NSGS mouse (left) compared with the larger spleen of a *C. bovis* PCR-negative CMML PDX-recipient NSGS mouse (right) that received the same PDX.

CMML CD45<sup>+</sup> cellular infiltrates in the bone marrow of PDX-recipient *C. bovis* PCR-negative mice impaired murine platelet formation, resulting in greater ( $P = 0.0192$ ) thrombocytopenia than that of PDX-recipient *C. bovis* PCR-positive mice. CMML CD45<sup>+</sup> cellular infiltrates in the spleen of PDX-recipient *C. bovis* PCR-negative mice resulted in greater ( $P = 0.0150$ ) splenomegaly than that in *C. bovis* PCR-positive mice. Indeed, the spleen of an individual PDX-recipient *C. bovis* PCR-negative mouse weighed substantially more than that of a *C. bovis* PCR-positive mouse that received the same PDX mononuclear cell isolate from the same CMML donor patient. The *C. bovis* PCR-positive PDX-recipient cohort had more circulating neutrophils than the *C. bovis* PCR negative cohort ( $P = 0.0002$ ), perhaps attributable to *C. bovis* skin colonization, a resulting cutaneous dysbiosis, and epithelial elicited antimicrobial proteins driving systemic inflammation.<sup>8,14</sup> However, this proposed mechanism requires experimental confirmation. Due to *C. bovis* infection, engraftment of CMML mononuclear cells among PDX-recipient NSGS mice was significantly diminished. These novel findings document for the first time that the integrity of preclinical research data obtained by using immunodeficient strains is measurably jeopardized by *C. bovis* infection. Immunodeficient mice become persistently infected with *C. bovis* and can either develop clinically apparent hyperkeratosis and alopecia or can remain asymptomatic and serve as persistently shedding reservoirs of the microbe.<sup>3,4,16-18,27</sup> *C. bovis* should be excluded from and not tolerated when detected in murine research facilities housing immunodeficient strains.

Murine biosecurity critically relies on the realization that—despite the absence of morbidity attributable to *C. bovis*—the organism may be present, can be PCR-detected, and is harbored by several clinically unaffected immunodeficient strains.<sup>18</sup> *C. bovis* is even transiently PCR-detectable among immunocompetent strains and is broadly PCR-detectable on room and equipment surfaces during a clinical outbreak.<sup>18</sup> An ‘active-closed’ method of VHP sterilization of housing equipment and rooms is an important component to successful facility-wide eradication of *C. bovis* and for mitigating the prevalence of other opportunistic microbes.<sup>1,24,25</sup> Despite *C. bovis* being among the more egregious of opportunistic outbreaks affecting immunodeficient

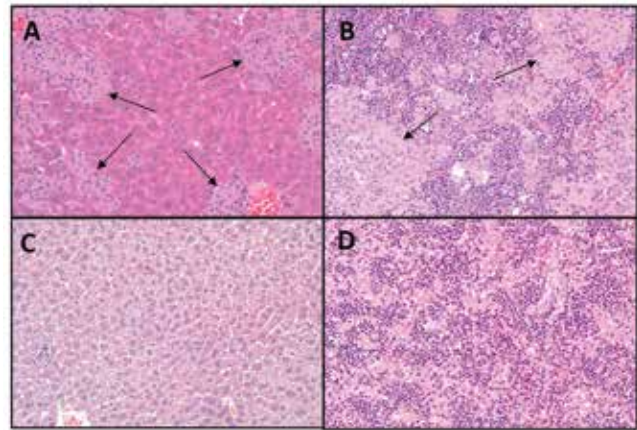


**Figure 5.** Histopathologic appearance of the CMML blasts and dysplastic binucleated cells (arrows) infiltrating the (A) liver and (B) spleen of *C. bovis* PCR-negative CMML PDX-recipient NSGS mice compared with the rare CMML infiltrates evident in the (C) liver and (D) spleen of *C. bovis* PCR-positive CMML PDX-recipient NSGS mice. Hematoxylin and eosin stain; magnification, 100 $\times$ .

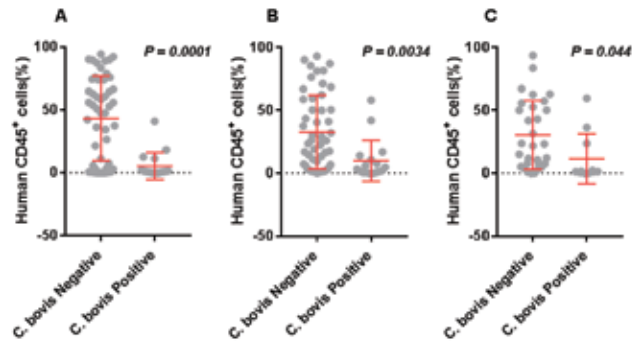


**Figure 6.** Percentage of human CD45<sup>+</sup> cells in isolates from the (A) spleen, (B) bone marrow, and (C) peripheral blood of *C. bovis* PCR-negative or -positive CMML PDX-recipient NSGS cohorts.

mice and although 58% of cancer center respondents confirm experiencing a case of *C. bovis* hyperkeratosis in immunodeficient mice, most facilities (74%) do not test or attempt to characterize the extent of environmental contamination caused by a clinical case of *C. bovis* hyperkeratosis. Nor do most cancer centers routinely PCR survey the environment or murine inventories for early evidence of *C. bovis* prior to its clinical manifestation. Nor do cancer centers broadly VHP decontaminate the *C. bovis*-affected facility space after an outbreak. Without appropriate biosecurity measures in place, recurrence of *C. bovis* infection, variability in preclinical data, and invalidation of studies involving immunodeficient mice are likely.<sup>18</sup>

Our prior attempts to cull and quarantine followed by decontamination without VHP only the presumed affected housing room and its equipment did not prevent *C. bovis* recurrence.<sup>18</sup> Two of the respondent cancer centers in the present survey indicated a willingness to rely “on the wishes of the investigator” regarding whether to treat, cull, or quarantine mice clinically affected by *C. bovis*. However, our experience indicates that even asymptomatic *C. bovis* PCR-positive immunodeficient mice shed *C. bovis*-infected keratin flakes, which are spread airborne through by fomite transmission, resulting in broad facility contamination, establishing niduses of recurrence, long before clinically apparent *C. bovis* hyperkeratosis manifests.<sup>3-6,15-18,27</sup> By the time *C. bovis* hyperkeratosis becomes clinically recognized

in an immunodeficient mouse, the organism is already broadly PCR-detectable in murine inventory, in the interior of the IVC rack exhaust plenum and in the air-handling unit, on neighboring equipment surfaces, on core imaging equipment, and on shared computer keyboards.<sup>18</sup> In addition, our current findings documenting diminished CMML engraftment due to *C. bovis* cutaneous infection of immunodeficient mice suggests that research data collected from even an asymptomatic *C. bovis* PCR-positive immunodeficient cohort may no longer be reliable and the study no longer valid. Consequently, attending veterinarians should consider immediately culling *C. bovis* clinically affected mice; culling *C. bovis* PCR-positive immunodeficient mice; broadly PCR-testing the facility environment, equipment, and murine inventory; and VHP sterilizing all rooms and equipment to prevent *C. bovis* recurrence.

As immunodeficient mice become more prevalent and because expectations persist for achieving reproducible results in ever-increasingly complex mouse model settings,<sup>11,28</sup> murine facilities must minimize the risk of opportunistic infections that invalidate research.<sup>18,25</sup> In the 17 mo (as of this report) since eradicating *C. bovis* program-wide and implementing comprehensive PCR environmental and murine monitoring and facility-wide VHP sterilization,<sup>18</sup> no environmental or murine specimen has tested *C. bovis* PCR-positive. The present report demonstrates how *C. bovis* infection of immunodeficient mice, although perhaps a cutaneous opportunistic pathogen, can alter CMML engraftment in a PDX mouse model and jeopardize research outcomes. Murine facilities should routinely PCR test for *C. bovis*, and VHP sterilize all equipment and rooms at regular intervals to prevent *C. bovis* recurrence.<sup>18,24,25</sup>

## Acknowledgments

We appreciate the contributions made by the Comparative Medicine Core and Survey Methods Core staff, support from the Flow Cytometry Core Facility at Moffitt Cancer Center, and the survey responses provided by cancer center attending veterinarians.

## References

1. Abdel-Wahab O, Gao J, Adli M, Dey A, Trimarchi T, Chung YR, Kuscus C, Hricik T, Ndiaye-Lobry D, Lafave LM, Koche R, Shih AH, Guryanova OA, Kim E, Li S, Pandey S, Shin JY, Telis L, Liu J, Bhatt PK, Monette S, Zhao X, Mason CE, Park CY, Bernstein BE, Aifantis I, Levine RL. 2013. Deletion of *Asxl1* results in myelodysplasia and severe developmental defects in vivo. *J Exp Med* 210:2641–2659. <https://doi.org/10.1084/jem.20131141>.
2. Arber DA, Orazi A, Hasserjian R, Thiele J, Borowitz MJ, Le Beau MM, Bloomfield CD, Cazzola M, Vardiman JW. 2016. The 2016 revision to the World Health Organization classification of myeloid neoplasms and acute leukemia. *Blood* 127:2391–2405. <https://doi.org/10.1182/blood-2016-03-643544>.
3. Burr HN, Lipman NS, White JR, Zheng J, Wolf FR. 2011. Strategies to prevent, treat, and provoke *Corynebacterium*-associated hyperkeratosis in athymic nude mice. *J Am Assoc Lab Anim Sci* 50:378–388.
4. Burr HN, Wolf FR, Lipman NS. 2012. *Corynebacterium bovis*: epizootologic features and environmental contamination in an enzootically infected rodent room. *J Am Assoc Lab Anim Sci* 51:189–198.
5. Clifford CB, Walton BJ, Reed TH, Coyle MB, White WJ, Amyx HL. 1995. Hyperkeratosis in athymic nude mice caused by a coryneform bacterium: microbiology, transmission, clinical signs, and pathology. *Lab Anim Sci* 45:131–139.
6. Field K, Greenstein G, Smith M, Herrman S, Gizzi J. 1995. Hyperkeratosis-associated coryneform in athymic nude mice. *Lab Anim Sci* 45:469.
7. Foreman O, Kavirayani AM, Griffey SM, Reader R, Shultz LD. 2011. Opportunistic bacterial infections in breeding colonies of the NSG mouse strain. *Vet Pathol* 48:495–499. <https://doi.org/10.1177/0300985810378282>.
8. Gallo RL, Hooper LV. 2012. Epithelial antimicrobial defense of the skin and intestine. *Nat Rev Immunol* 12:503–516. <https://doi.org/10.1038/nri3228>.
9. Hunter AM, Zhang L, Padron E. 2018. Current management and recent advances in the treatment of chronic myelomonocytic leukemia. *Curr Treat Options Oncol* 19:67–81. <https://doi.org/10.1007/s11864-018-0581-6>.
10. Itzykson R, Kosmider O, Renneville A, Gelsi-Boyer V, Meggen-dorfer M, Morabito M, Berthon C, Adès L, Fenaux P, Beyne-Rauzy O, Vey N, Braun T, Haferlach T, Dreyfus F, Cross NC, Preudhomme C, Bernard OA, Fontenay M, Vainchenker W, Schnittger S, Birnbaum D, Droin N, Solary E. 2013. Prognostic score including gene mutations in chronic myelomonocytic leukemia. *J Clin Oncol* 31:2428–2436. <https://doi.org/10.1200/JCO.2012.47.3314>.
11. Justice MJ, Dhillon P. 2016. Using the mouse to model human disease: increasing validity and reproducibility. *Dis Model Mech* 9:101–103. <https://doi.org/10.1242/dmm.024547>.
12. Kim E, Ilagan JO, Liang Y, Daubner GM, Lee SC, Ramakrishnan A, Li Y, Chung YR, Micol JB, Murphy ME, Cho H, Kim MK, Zebari AS, Aumann S, Park CY, Buonamici S, Smith PG, Deeg HJ, Lobry C, Aifantis I, Modis Y, Allain FH, Halene S, Bradley RK, Abdel-Wahab O. 2015. SRSF2 mutations contribute to myelodysplasia by mutant-specific effects on exon recognition. *Cancer Cell* 27:617–630. <https://doi.org/10.1016/j.ccell.2015.04.006>.
13. Klinakis A, Lobry C, Abdel-Wahab O, Oh P, Haeno H, Buonamici S, van De Walle I, Cathelin S, Trimarchi T, Araldi E, Liu C, Ibrahim S, Beran M, Zavadil J, Efstratiadis A, Taghon T, Michor F, Levine RL, Aifantis I. 2011. A novel tumour-suppressor function for the Notch pathway in myeloid leukaemia. *Nature* 473:230–233. <https://doi.org/10.1038/nature09999>.
14. Kobayashi T, Glatz M, Horiuchi K, Kawasaki H, Akiyama H, Kaplan DH, Kong HH, Amagai M, Nagao K. 2015. Dysbiosis and *Staphylococcus aureus* colonization drives inflammation in atopic dermatitis. *Immunity* 42:756–766. <https://doi.org/10.1016/j.immuni.2015.03.014>.
15. Manuel CA, Pugazhenth U, Leszczynski JK. 2016. Surveillance of a ventilated rack system for *Corynebacterium bovis* by sampling exhaust-air manifolds. *J Am Assoc Lab Anim Sci* 55:58–65.
16. Manuel CA, Bagby SM, Reisinger JA, Pugazhenth U, Pitts TM, Keysar SB, Arcaroli JJ, Leszczynski JK. 2017. Procedure for horizontal transfer of patient-derived xenograft tumors to eliminate *Corynebacterium bovis*. *J Am Assoc Lab Anim Sci* 56:166–172.
17. Manuel CA, Pugazhenth U, Spiegel SP, Leszczynski JK. 2017. Detection and elimination of *Corynebacterium bovis* from barrier rooms by using an environmental sampling surveillance program. *J Am Assoc Lab Anim Sci* 56:202–209.
18. Miedel EL, Ragland NH, Engelman RW. 2018. Facility-wide eradication of *Corynebacterium bovis* by using PCR-validated vaporized hydrogen peroxide. *J Am Assoc Lab Anim Sci* 57:465–476. <https://doi.org/10.30802/AALAS-JAALAS-17-000135>.
19. Moran-Crusio K, Reavie L, Shih A, Abdel-Wahab O, Ndiaye-Lobry D, Lobry C, Figueroa ME, Vasanthakumar A, Patel J, Zhao X, Perna F, Pandey S, Madzo J, Song C, Dai Q, He C, Ibrahim S, Beran M, Zavadil J, Nimer SD, Melnick A, Godley LA, Aifantis I, Levine RL. 2011. Tet2 loss leads to increased hematopoietic stem cell self-renewal and myeloid transformation. *Cancer Cell* 20:11–24. <https://doi.org/10.1016/j.ccr.2011.06.001>.
20. Padron E, Painter JS, Kunigal S, Mailloux AW, McGraw K, McDaniel JM, Kim E, Bebbington C, Baer M, Yarranton G, Lancet J, Komrokji RS, Abdel-Wahab O, List AF, Epling-Burnette PK. 2013. GM-CSF-dependent pSTAT5 sensitivity is a feature with therapeutic potential in chronic myelomonocytic leukemia. *Blood* 121:5068–5077. <https://doi.org/10.1182/blood-2012-10-460170>.
21. Padron E, Garcia-Manero G, Patnaik MM, Itzykson R, Lasho T, Nazha A, Rampal RK, Sanchez ME, Jabbour E, Al Ali NH, Thompson Z, Colla S, Fenaux P, Kantarjian HM, Killick S, Sekeres MA, List AF, Onida F, Komrokji RS, Tefferi A, Solary E. 2015. An international data set for CMML validates prognostic

- scoring systems and demonstrates a need for novel prognostication strategies. *Blood Cancer J* 5:e333. <https://doi.org/10.1038/bcj.2015.53>.
22. **Patnaik MM, Itzykson R, Lasho TL, Kosmider O, Finke CM, Hanson CA, Knudson RA, Ketterling RP, Tefferi A, Solary E.** 2014. ASXL1 and SETBP1 mutations and their prognostic contribution in chronic myelomonocytic leukemia: a 2-center study of 466 patients. *Leukemia* 28:2206–2212. <https://doi.org/10.1038/leu.2014.125>.
  23. **Quivoron C, Couronné L, Della Valle V, Lopez CK, Plo I, Wagner-Ballon O, Do Cruzeiro M, Delhommeau F, Arnulf B, Stern MH, Godley L, Opolon P, Tilly H, Solary E, Duffourd Y, Dessen P, Merle-Beral H, Nguyen-Khac F, Fontenay M, Vainchenker W, Bastard C, Mercher T, Bernard OA.** 2011. TET2 inactivation results in pleiotropic hematopoietic abnormalities in mouse and is a recurrent event during human lymphomagenesis. *Cancer Cell* 20:25–38. <https://doi.org/10.1016/j.ccr.2011.06.003>.
  24. **Ragland NH, Miedel EL, Gomez JM, Engelman RW.** 2017. *Staphylococcus xylosus* PCR-validated decontamination of murine individually ventilated cage racks and air handling units by using ‘active-closed’ exposure to vaporized hydrogen peroxide. *J Am Assoc Lab Anim Sci* 56:742–751.
  25. **Ragland NH, Miedel EL, Engelman RW.** 2019. pcr prevalence of murine opportunistic microbes and their mitigation by using vaporized hydrogen peroxide. *J Am Assoc Lab Anim Sci* 58:208–215.
  26. **Santagostino SF, Arbona RJR, Nashat MA, White JR, Monette S.** 2017. Pathology of aging in NOD scid  $\gamma$  female mice. *Vet Pathol* 54:855–869. <https://doi.org/10.1177/0300985817698210>.
  27. **Scanziani E, Gobbi A, Crippa L, Giusti AM, Giavazzi R, Cavalletti E, Luini M.** 1997. Outbreaks of hyperkeratotic dermatitis of athymic nude mice in northern Italy. *Lab Anim* 31:206–211. <https://doi.org/10.1258/002367797780596310>.
  28. **Servick K.** 2016. Of mice and microbes. *Science* 353:741–743. <https://doi.org/10.1126/science.353.6301.741>.
  29. **Treuting PM, Clifford CB, Sellers RS, Brayton CF.** 2011. Of mice and microflora: considerations for genetically engineered mice. *Vet Pathol* 49:44–63. <https://doi.org/10.1177/0300985811431446>.
  30. **Wunderlich M, Chou FS, Link KA, Mizukawa B, Perry RL, Carroll M, Mulloy JC.** 2010. AML xenograft efficiency is significantly improved in NOD/SCID-IL2RG mice constitutively expressing human SCF, GM-CSF and IL3. *Leukemia* 24:1785–1788. <https://doi.org/10.1038/leu.2010.158>.
  31. **Yoshimi A, Balasis ME, Vedder A, Feldman K, Ma Y, Zhang H, Lee SC, Letson C, Niyongere S, Lu SX, Ball M, Taylor J, Zhang Q, Zhao Y, Youssef S, Chung YR, Zhang XJ, Durham BH, Yang W, List AF, Loh ML, Klimek V, Berger MF, Stieglitz E, Padron E, Abdel-Wahab O.** 2017. Robust patient-derived xenografts of MDS/MPN overlap syndromes capture the unique characteristics of CMML and JMML. *Blood* 130:397–407. <https://doi.org/10.1182/blood-2017-01-763219>.